

EFFECT OF MATERIAL MODELS ON NUMERICAL RESULT OF A FLEXURE-SHEAR-CRITICAL RC COLUMN

Wencong LI*1

ABSTRACT

Predicting the inelastic hysteretic behavior of shear-critical or flexure-shear-critical RC columns still remains challenging. In this paper, two numerical modelling methods for a flexure-shear-critical RC column are evaluated. One is based on fiber-section element with lumped shear spring characterized by shear limit curve in OpenSees; the effects of hysteretic behavior for longitudinal reinforcement on the numerical results are investigated. The other is modelled with continuum element based on the MCFT/DSFM using VecTor2. Both methods can predict the shear-related hysteretic behavior of the RC column, if appropriate models are provided.

Keywords: flexure-shear-critical RC column, material model, OpenSees, shear limit curve, VecTor2

1. INTRODUCTION

For the evaluation of the cyclic behavior of shear-critical RC columns, experimental test can be the most reliable source. However, in many practical problems, it is very difficult and costly to test actual specimens. Instead, numerical models are used to capture the nonlinear behavior of structural elements. Even though there has been many years of experimental and analytical investigations, replicating the hysteretic behavior of flexure-shear-critical RC column is still a very challenging task. In this paper, two numerical modelling methods for a flexure-shear-critical RC column are evaluated. One is modelled with OpenSees[1]. In OpenSees, fiber-section element with lumped shear spring at the end is used, and the effects of hysteretic behavior for longitudinal reinforcement on the numerical results are investigated. The other is modelled with continuum element using VecTor2[2]. In concrete models of VecTor2, the behaviors of compression softening, tension stiffening and tension softening are considered. Both numerical modelling methods can predict the shear-related hysteretic behavior of the RC column, if appropriate models are provided.

2. SPECIMEN

A RC column specimen with poor transverse reinforcement is investigated in this study through numerical analysis. The experimental parameters of the specimen are summarized in Table 1. The mechanical properties of reinforcement bars used in this specimen are listed in Table 2. The dimensions and reinforcement properties of the

Table 2 Mechanical properties of reinforcement

Reinforcement	a (cm ²)	f_y (MPa)	ϵ_y (%)	E_s (GPa)	
Rebar	D13	1.27	346	0.19	187
Hoop	4 ϕ	0.13	199	0.10	197

Note : a = cross-sectional area, f_y = yield strength of steel, ϵ_y = yield strain of steel, E_s = modulus of elasticity.

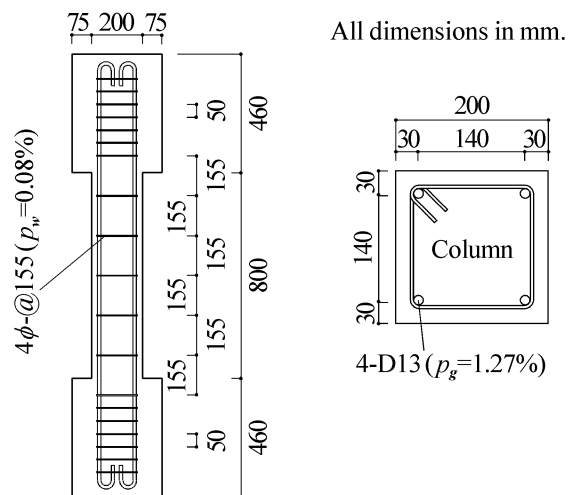


Fig. 1 Dimensions and reinforcement properties

specimen are illustrated in Fig. 1. The specimen has a sectional dimension of 200 mm × 200 mm and clear height of 800 mm. The shear span to depth ratio of the column is 2.0. Four D13 reinforcement bars are used as longitudinal reinforcement with a longitudinal reinforcement ratio, p_g , of 1.33%. Transverse reinforcement bars consist of 4 bars spaced at 155 mm interval (transverse reinforcement ratio, p_w = 0.08%). Cyclic lateral displacements are applied to the specimen without applying axial load.

Table 1 Experimental parameters

RC column specimen	$M/(Q \cdot D) = 2.0$, Concrete compressive strength $\sigma_B = 26.7$ MPa, Axial force ratio $N/(b \cdot D \cdot \sigma_B) = 0$, Rebar : 4-D13 ($p_g = 1.27\%$), Hoop : 4 ϕ -@155 ($p_w = 0.08\%$).
--------------------	-----------------------------------------------------------------------------------------------------------------------------------------------------------------------------------------------------------------------------

*1 Assistant Prof., Fac. of Eng., Dept. of Arch., Fukuoka University, Dr. Eng., JCI Member

3. EXPERIMENTAL RESULTS

Crack patterns of the specimen at the drift ratio, R , of 0.5%, 1.0% and 1.5% are illustrated in Fig. 2. The relationship between the experimental lateral force, Q , and R of the specimen is shown in Fig. 3. The relationship between the average axial strain, ε_v , and R of this specimen is also shown in this Figure. In the Q - R curve, the dotted lines represent the calculated flexural strength of column V_f based on the simplified equation of AIJ[3], and the solid lines represent the calculated shear strength of column V_u using the equation proposed by Sezen[4]. The shear strength expression of the model is divided into two terms: the shear carried by concrete, V_c ; and the shear carried by transverse reinforcement through a 45° truss model, V_s . The V_u is defined as follows:

$$V_u = k(V_c + V_s)$$

$$= k \frac{6\sqrt{f'_c}}{a/d} \sqrt{1 + \frac{N}{6A_g\sqrt{f'_c}}} 0.8A_g + k \frac{A_s \cdot f_{yw} \cdot d}{s} \quad (1)$$

where,

- f'_c : concrete compressive strength
- N : axial load on the column
- A_g : gross concrete area of the column
- a : distance from maximum moment to the inflection point
- d : effective depth of the column
- A_s : area of the transverse reinforcement
- f_{yw} : yield strength of the transverse reinforcement
- s : spacing of the transverse reinforcement
- k : degradation coefficient of the shear strength

When the drift ratio R was approximately 0.5%, flexural cracks were observed at both ends of the column, and then oblique cracks occurred. Rebars around critical sections of the column yielded when the drift ratio approached 1.0%. At yielding, the experimental lateral capacity, which was 41.2kN, exceeded the calculated flexural strength of column V_f . Due to the poor transverse reinforcement and degradation of shear strength with

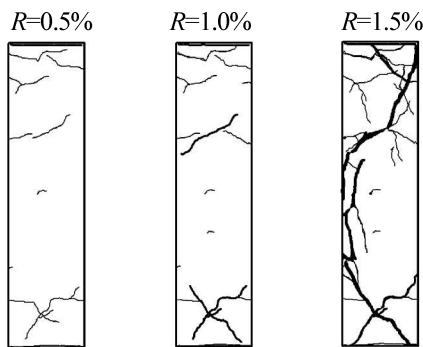


Fig. 2 Observed cracking patterns of column along depth side surface

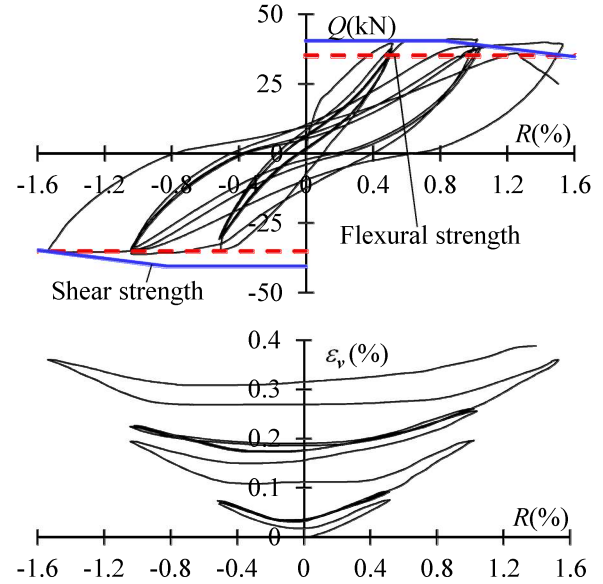


Fig. 3 Measured Q - R and ε_v - R relationships

increasing displacement ductility, the column failed in shear during the second load cycle of $R=1.5\%$ (see Fig. 3). Because no axial force was applied to the column, the variation of average axial strain ε_v of this specimen was not significant when shear failure occurred.

4. NUMERICAL MODELLING WITH OPENSEES

This chapter describes a nonlinear numerical study on the tested specimen based on OpenSees. OpenSees is a software framework for simulating the seismic response of structural and geotechnical systems. It has been developed as the computational platform for research in performance-based earthquake engineering at the Pacific Earthquake Engineering Research Center.

Fig. 4 illustrates the numerical element of the specimen in OpenSees. The numerical element consists of a

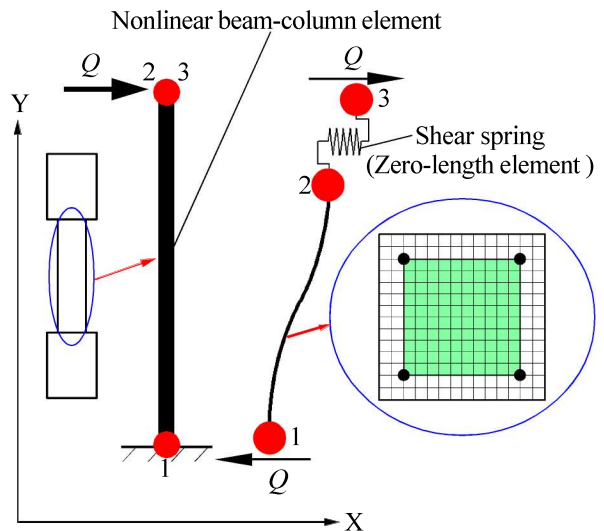


Fig. 4 Numerical element of 09-C (OpenSees)

two-dimensional nonlinear beam-column with fiber sections located at the integration points. Each section is subdivided into a number of fibers where each fiber is under uniaxial state of stress. The specimen is modelled with three nodes and each node has three degrees-of-freedom. Node 1 is fully fixed, and node 3 is constrained on rotation only. In order to capture shear strength degradation, a shear spring is modelled between nodes 2 and 3 utilizing zero-length element (see Fig. 4). The shear spring is defined with the limit state material and the shear limit curve based on the work of Elwood and Moehle[5]. Note that the vertical translation and rotational degrees of freedoms (DOFs) of node 2 are constrained with the DOFs of node 3.

The concrete behavior is simulated with the nonlinear Concrete04 material in which the envelope of the compressive stress-strain response is defined using the model proposed by Mander et al.[6]. In this model, for unloading and reloading in compression, the Karsan-Jirsa model[7] is used to determine the slope of the curve. The tensile strength of concrete f_{cr} (negative value refers to compression) is defined by the following expression:

$$f_{cr} = 0.33\sqrt{-\sigma_B} \quad (2)$$

where,
 σ_B : concrete compressive strength (in MPa)

For tensile loading, an exponential curve is used to define the envelope to the stress-strain curve. For unloading and reloading in tension, the secant stiffness is used to define the path. The corresponding hysteretic stress-strain relation is illustrated in Fig. 5.

For longitudinal reinforcement, two models are selected to evaluate the numerical response of the specimen. One is Steel02 material which is a uniaxial Giuffre-Menegotto-Pinto steel material object without isotropic strain hardening. This model is popular for steel in OpenSees and the corresponding hysteretic behavior is shown in Fig. 6. The other is hysteretic material which has seldom been chosen for longitudinal reinforcement. The skeleton curve is defined as tri-linear response which is based on the result of tensile test. The corresponding hysteretic behavior is shown in Fig. 7. In the hysteretic material model, pinching of stress and strain, damage due to ductility and energy, and degraded unloading stiffness based on ductility can be considered. In

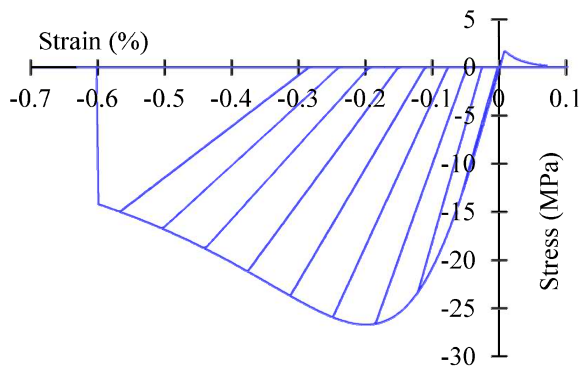


Fig. 5 Hysteretic stress-strain relation of Concrete04 model in tension-compression (Mander et al. model)

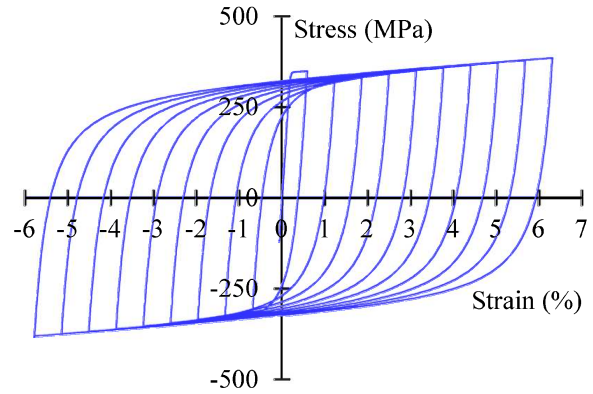


Fig. 6 OpenSees Steel02 model for rebar

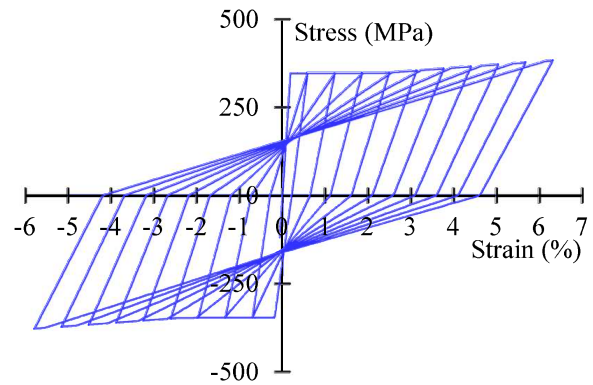


Fig. 7 OpenSees Hysteretic model for rebar

this study, in order to improve precision of numerical response, damage due to ductility and energy, and degraded unloading stiffness based on ductility are considered. Further details of concrete and steel models can be investigated in the OpenSees's manual[8].

Five integration points along the nonlinear beam-column element are defined. Perfect bond model is assumed between the bar and concrete element. The modified Newton solution algorithm is used to solve nonlinear equations.

The static cyclic analysis is carried out by imposing lateral displacements to node 3 based on the displacement history applied to the tested specimen. The comparisons of experimental results and numerical results are shown in Fig. 8. The stress-strain relations of a rebar at the top end of the column (one of the critical sections) are provided in Fig. 9. For both cases (Steel02 model and Hysteretic model), the stress of rebar at the top end of the column has reached the yield strength (see Fig. 9). And, shear failure can be detected when the drift ratio, R , is a little greater than 1.2% (see Fig. 8). The detection of shear failure is related to modelling the shear spring and shear limit curve. However, for Steel02 model, the divergence is significant after detection of shear failure, and the numerical $Q-R$ relationship and stress- R curve of the longitudinal reinforcement are too plump. On the other hand, the response of $Q-R$ relationship of numerical model for Hysteretic model matches the experimental result closer than that of Steel02, because damage due to ductility and energy, and degraded unloading stiffness based on ductility are considered in Hysteretic model. It is verified that the numerical response of OpenSees is closely related to the hysteretic behavior of longitudinal reinforcement.

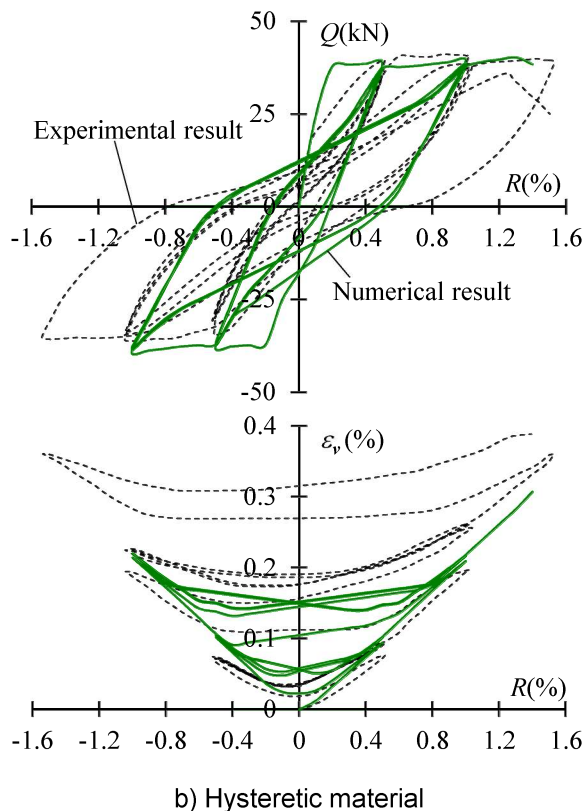
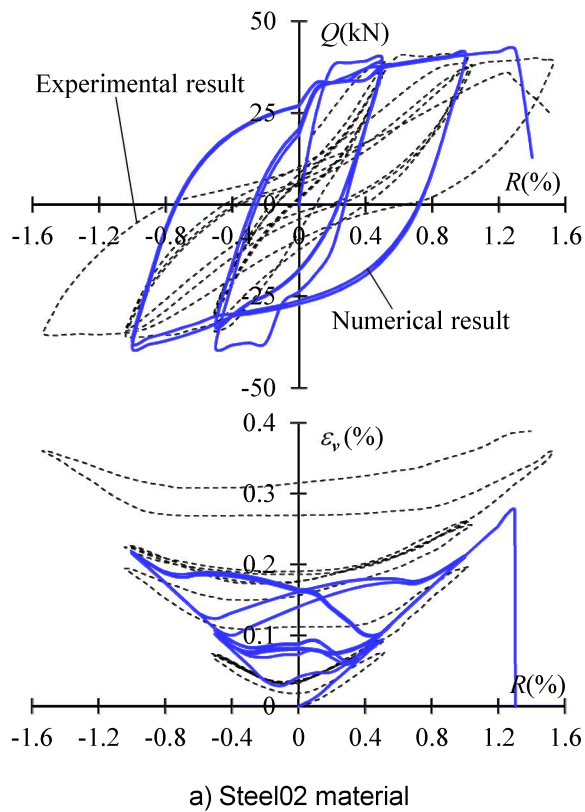


Fig. 8 Comparisons of experimental results and numerical results (OpenSees)

However, in this study, the flexural stiffness based on OpenSees is higher than that of the experimental one right after the elastic region, because OpenSees does not consider the load-deformation behavior of cracked reinforced concrete

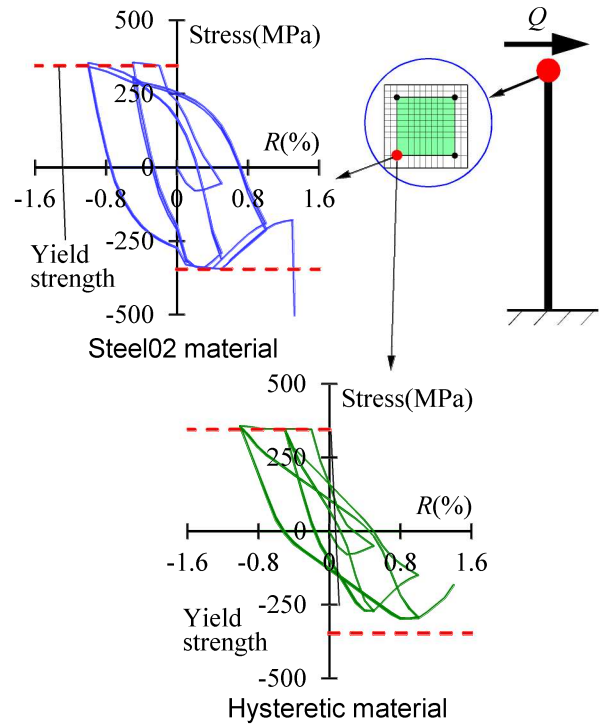


Fig. 9 Numerical results of stress of longitudinal reinforcement (OpenSees)

subjected to shear.

5. NUMERICAL MODELLING USING VECTOR2

This chapter describes a nonlinear numerical study on the tested specimen based on VecTor2. VecTor2 is a nonlinear finite element program for the analysis of two-dimensional reinforced concrete structures and has been developed at University of Toronto. The theoretical bases of VecTor2 are the Modified Compression Field Theory (MCFT)[9] and the Disturbed Stress Field Model (DSFM)[10]. VecTor2 permits relative accurate assessments of structural performance (strength, post-peak behavior, failure mode, deflections and cracking) of RC elements. The Vector2 bundle includes: FormWorks, a graphics-based preprocessor program that simplifies the model building; Augustus, a complete VecTor2 post-processor that may provide all the global and local results in useful numeric or graphic formats. It is also able to display the specimen crack pattern at each stage of imposed displacement. However, in order to predict the accurate numerical response of a shear-flexural-critical RC column, using appropriate material models for concrete elements, reinforcement elements and analytical models for each material is essential.

The automatic mesh generation facility with the hybrid discretization type is used to create the mesh of the specimen as shown in Fig. 10. In this model, the specimen is represented with rectangular elements for the concrete and truss bar elements for the longitudinal reinforcing bars. The maximum size of coarse aggregate is considered as the default value of VecTor2. Nodes at the bottom end of the column are restrained in both X and Y directions. However, all the other nodes are unconstrained. In order to constrain the rotation of upper stub and prevent localized failure where

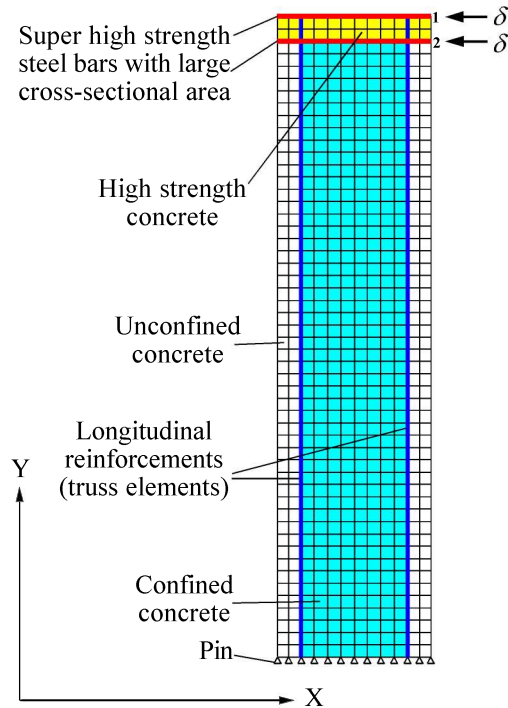


Fig. 10 FormWorks model

Table 3 Analysis parameters of VecTor2

Compression base curve	Popovics (NSC)
Compression post-peak	Popovics / Mander
Compression softening	Vecchio 1992-A
Tension stiffening	Modified Bentz
Tension softening	Linear
Concrete hysteresis	Nonlinear w/ Plastic Offsets
Concrete dilatation	Variable - Kupfer
Cracking criterion	Mohr-Coulomb (stress)
Crack stress calculation	Basic (DSFM/MCFT)
Concrete bond	Perfect bond
Rebar stress-strain response	Linear strain-hardening (Trilinear)
Rebar hysteresis	Giuffre-Menegotto-Pinto
Rebar buckling	Not considered

the displacement load is applied, the upper stub is modelled with high strength concrete reinforced by two super high strength steel bars with large cross-sectional area, and lateral displacements δ are applied to node 1 and node 2 simultaneously.

In this study, two reinforced concrete material types are used for the column region. One type represents the unconfined concrete. The other type models the confined concrete. Confinement effects are taken into account by means of the geometric percentage of in-plane and out-of-plane reinforcements[11] for confined concrete elements. With regard to concrete models, the Popovics (Normal Strength Concrete) model is selected for the pre-peak compression response and the Popovics / Mander model is

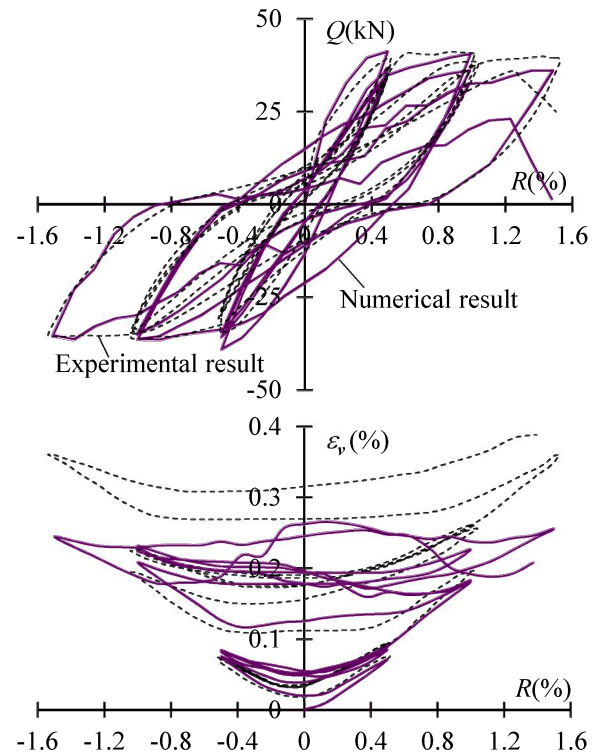


Fig. 11 Comparison of experimental results and numerical results of VecTor2

selected for the post-peak compression response, together with the Vecchio 1992-A compression softening model[12]. The Bentz 2003 model is selected for tension stiffening and tension softening behavior is assumed to be linear response. For reinforcement model, the skeleton curve is the same with the backbone of Fig. 7 and Giuffre-Menegotto-Pinto model is selected for the hysteretic response. In this study, the bond material is assigned a numerically large stiffness and strength to avoid bond failure. Summation of the material properties for the concrete elements, reinforcement elements, bond elements, and the chosen analytical models for each material are listed in Table 3. Further details of concrete and steel models can be investigated in the VecTor2 & Formworks User's Manual[11].

Based on the numerical model as mentioned above, the results from the VecTor2 are shown in Fig. 11. Fig. 12 presents the deformed shape and crack distribution of the column at drift ratios of 0.5% and 1.5%, respectively. The stress of longitudinal reinforcement vs. drift ratio response of a rebar at the top end of the column is presented in Fig. 13. The flexural stiffness based on VecTor2 almost agrees with the experimental one. This response is more accurate than the numerical result based on OpenSees, because VecTor2 considers the load-deformation behavior of cracked reinforced concrete subjected to shear. The changing of ϵ_v for numerical model leans toward the same tendency with the response of tested column before R is less than 1.0%. At the drift ratio of 0.5%, many small flexural cracks and some large shear cracks developed. At the drift ratio of 1.5%, the number of large shear cracks increase significantly, the crushing of concrete elements is predicted. This demonstrates the column fails in a shear manner. Moreover,

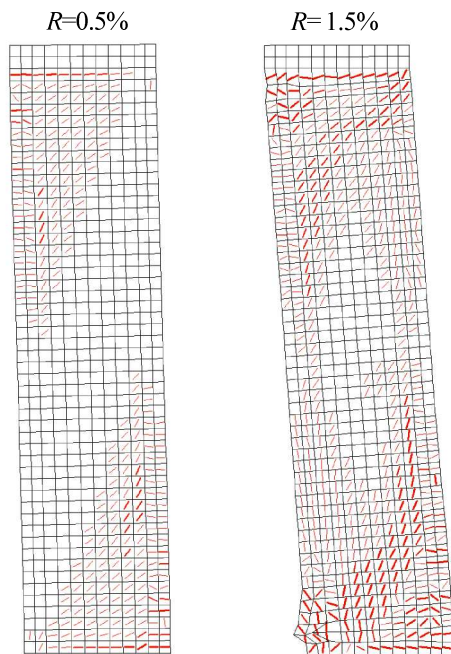


Fig. 12 Combined view of displacement and crack direction in depth side by VecTor2

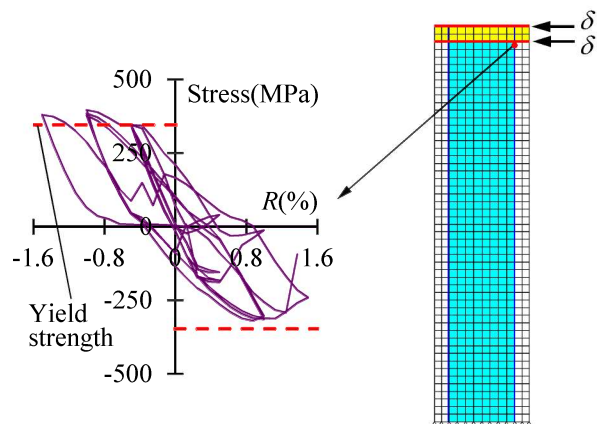


Fig. 13 Numerical result of stress of longitudinal reinforcement (VecTor2)

the numerical result in Fig. 13 indicates the stress of rebar at the top end of the column has reached the yield strength. VecTor2 does not require assumptions on shear spring, and the modelling approach can be applied to more general configuration of geometry and reinforcement layout. The program could successfully predict the behavior of shear-flexural-critical column if appropriate combination of material models and analytical models is provided. However, modelling of a RC element with finite element in VecTor2 requires more computing time than other lumped spring approaches.

6. CONCLUSIONS

The numerical studies of the tested specimen lead to the following conclusions:

(1) It is possible to detect shear failure of the specimen using OpenSees by introducing shear spring element and shear limit curve. The model with shear spring, which was empiri-

cally calibrated, is computationally efficient.

(2) The numerical response of OpenSees is closely related to the hysteretic behavior of longitudinal reinforcement. And, the response of numerical model for Hysteretic model matches the experimental result closer than that of Steel02 model, because damage due to ductility and energy, and degraded unloading stiffness based on ductility can be considered in Hysteretic model.

(3) The response of flexural stiffness based on VecTor2 is more accurate than the numerical result based on OpenSees because VecTor2 considers the load-deformation behavior of cracked reinforced concrete subjected to shear.

(4) VecTor2 can successfully predict the behavior of shear-flexural-critical column if appropriate combination of material models and analytical models is provided.

ACKNOWLEDGEMENT

The author would like to express his appreciation to Assistant Professor Oh-Sung Kwon at University of Toronto for his considerable assistance, and would like to thank Professor F.J. Vecchio at University of Toronto for providing VecTor2 software utilized for numerical study.

REFERENCES

- [1] The Regents of the University of California, OpenSees: Open System for Earthquake Engineering Simulation, Pacific Earthquake Engineering Research Center, <http://opensees.berkeley.edu>.
- [2] F.J. Vecchio, E.C. Bentz, M.P. Collins, Tools for forensic analysis of concrete structures. Computer and Concrete, Vol. 1, No. 1, pp. 1-14, 2004.
- [3] Architectural Institute of Japan (AIJ), "Ultimate Strength and Deformation Capacity Buildings in Seismic Design," AIJ, 1990 (In Japanese).
- [4] Halil Sezen, "Seismic behavior and modeling of reinforced concrete building columns," Ph.D. Thesis, Department of Civil and Environmental Engineering, University of California, Berkeley, United States of America.
- [5] Kenneth J. Elwood and Jack P. Moehle, "Shake Table Tests and Analytical Studies on the Gravity Load Collapse of Reinforced Concrete Frames," Pacific Earthquake Engineering Research Center, University of California, Berkeley, Calif. PEER Report 2003/01.
- [6] Mander, J. B., Priestley, M. J. N., and Park, R., "Theoretical stress-strain model for confined concrete," Journal of Structural Engineering ASCE, 114(8), pp. 1804-1826, 1988.
- [7] Karsan, I. D., and Jirsa, J. O., "Behavior of concrete under compressive loading," Journal of Structural Division ASCE, Vol 95, No. ST 12, Proc paper 6935, pp. 2543-2563, 23 FIG, 11, 1969.
- [8] Mazzoni, S., McKenna, F., Scott, M. H., et al. "OpenSees Command Language Manual," The Regents of the University of California, July 2007.
- [9] Vecchio, F.J. and Collins, M.P., "The Modified Compression Field Theory for Reinforced Concrete Elements Subject to Shear," ACI Journal Vol. 83, No. 2, pp. 219-231, 1986.
- [10] Vecchio, F.J., "Disturbed Stress Field Model for Reinforced Concrete: Formulation," ASCE Journal of Structural Engineering, Vol. 126, No. 9, pp. 1070-1077, 2000.
- [11] Wang, P.S., Vecchio, F.J. and Trommels, H. "VecTor2 & Formworks User's Manual (Second Edition)," VecTor Analysis Group C/O F.J. Vecchio, Department of Civil Engineering, University of Toronto, August 2013, <http://www.civ.utoronto.ca/vector>.
- [12] Vecchio, F.J. "Finite Element Modeling of Concrete Expansion and Confinement," ASCE Journal of Structural Engineering, Vol. 118, No. 9, pp. 2390-2406, 1992.